Use of CFD in the Design of the 10- by 10-Foot Supersonic Wind Tunnel Characterization Array

Aaron M. Johnson[1]
Jacobs Technology, NASA Glenn Research Center, Cleveland, Ohio, 44126, United States

Veronica Hawke[2]
STC, NASA Ames Research Center, Mountain View, California, 94043, United States

Nikki Parsons[3]
HX5 Sierra, NASA Glenn Research Center, Cleveland, Ohio, 44126, United States

At the 10- by 10-Foot Supersonic Wind Tunnel at the NASA Glenn Research Center, a future full test section characterization generated an ideal opportunity to design and build new characterization hardware to improve the understanding of the flow field, including flow quality, uniformity, and uncertainty in primary variables of interest. An array of flow sensing probes, referred to as the Characterization Array, was designed and built to replace 1960's-era test section characterization hardware. Many references exist to guide wind tunnel characterization practitioners in the design of new hardware to properly measure various aspects of the flow within their wind tunnel facilities. Although reliable sources of information, these references tend to be over 30 years old and are not exhaustive. In scenarios where design decisions needed to be validated, computational simulations of the flow field around the characterization hardware were used. Decisions regarding probe location, probe spacing, and performance of various probes were justified using computational fluid dynamic simulations and rules-of-thumb from the legacy resources available in literature. This paper is intended to serve as an example of the benefits from integrating CFD into the design of wind tunnel hardware, particularly hardware for wind tunnel characterization.

I. Nomenclature

C_d	=	drag coefficient
P_c	=	cone surface static pressure
$P_{T,2}$	=	post-normal-shock total pressure
$P_{T,4}$	=	post-oblique-shock, post-normal-shock total pressure on a supersonic wedge probe
RTD	=	resistance temperature detector
SWT	=	supersonic wind tunnel
VAW	=	variable-angle-wedge

[1] Wind Tunnel Characterization Lead Engineer, NASA Glenn Research Center (Jacobs, TFOME II), AIAA member.
[2] Senior Research Scientist, NASA Ames Research Center (STC), AIAA member.
[3] Wind Tunnel Characterization Engineer, NASA Glenn Research Center (HX5/Sierra, TFOME II), AIAA member.

II.Introduction

The 10- by 10-Foot Supersonic Wind Tunnel (10x10 SWT) at the NASA Glenn Research Center last underwent a full characterization effort between 1993 and 1995, during which a piece of hardware known as the 17-Wedge Array was used to acquire test section flow information. Since 1995, periodic test entries were performed to monitor the health of the tunnel calibration. Around 2017, the replacement of the facility data acquisition system was put onto the facility schedule, which necessitates a follow-up test section calibration. With nearly 30 years between the last full test section characterization and the upcoming one, the wind tunnel characterization team wanted to take advantage of this opportunity to fully characterize the facility. In 2020, a decision was made within the NASA Glenn wind tunnel characterization team to pursue a design for a new array of flow-sensing probes to improve the quality of the data which would be acquired during the upcoming full test section characterization[4].

Lessons learned from members of the Wind Tunnel Characterization Working Group[5] (WTCWG), a cross-agency working group supported by NASA Aerosciences Evaluation and Test Capabilities (AETC) Portfolio Office, were utilized in the initial design process along with recommended practice documents for wind tunnel calibration and flow measurements (Ref. [1,2,3,4]). Although these resources were very useful in preliminary design efforts, additional validation of design choices was desired to ensure potential sources of error are minimized for the various flow sensing probe types to be used with the new characterization hardware. Computational fluid dynamic (CFD) simulations during the 10x10 SWT Characterization Array design effort were supported by the AETC CFD Wind Tunnel Integration Project.

III. Background Information

A. Description of the 10- by 10-Foot Supersonic Wind Tunnel

The 10- by 10-Foot Supersonic Wind Tunnel at the NASA Glenn Research Center is a continuous-flow, variable-density wind tunnel. An overview of the tunnel loop is shown in Figure 1. The facility can be operated in either a closed-loop or an open-loop cycle. In the closed-loop cycle, the tunnel operates in a continuous-flow mode and the tunnel pressure level can be varied from 200 psf to 2.5 times standard atmospheric pressure (the full operating envelopes are given in Ref. [5]). The facility pressure level is controlled by a vacuum system used to lower the pressure within the tunnel shell. In the open-loop cycle, the tunnel operates at atmospheric pressure and in a single-pass model where the air is brought in through the air dryer, around the circuit through the test section, and exhausted out the muffler. The open-loop cycle is used for models that introduce contaminants into the airstream, such as the combustion products from an engine test, or when the facility air heater is used. The facility operating mode is controlled by the position of a 24-ft valve. The test section elevation view is shown in Figure 2. The upstream cross section of the test section is 10 feet wide by 10 feet high. The test section is 40 feet long and its walls diverge 0° 22’ to a width of 10.51 feet at the downstream end, whereas its floor and ceiling are parallel.

The facility’s calibrated Mach number range is 2.0 to 3.5 which can be achieved in both open-loop and closed-loop cycle. The airflow is moved through the facility by two drive systems, each consisting of a large axial-flow compressor powered by electric motors. The primary drive is used alone for Mach number conditions from 2.0 to 2.6. The primary drive is an eight-stage, axial-flow compressor powered by four 41,500-hp electric motors. For Mach numbers of 2.5 and greater, both primary and secondary drive systems are used. The secondary drive is a ten-stage, axial-flow compressor driven by three 41,500-hp electric motors. Mach numbers 2.5 and 2.6 can be achieved with or without using the second drive.

The test section Mach number is controlled by the mass flow generated by the drive systems and the position of the flexible-wall nozzle (flexwall). The flexwall consists of two 10-ft-high, 76-ft-long, and 1.375-in-thick stainless-steel plates positioned by hydraulically operated screwjacks. The positioning system incorporates cams on a common shaft; the cams have flats that correspond to 0.1 Mach number increments. The control system for the flexwall position was improved before the 1995 calibration to allow the flexwall to be set at off-design conditions, which allows for a nearly continuous Mach number range between 2.0 and 3.5. Reference [5] describes in more detail the facility and its operation.

[4] At the time of this report, the full characterization effort is scheduled for calendar year 2026.

[5] At the time of this report, membership of the WTCWG includes personnel from NASA Ames, Glenn, and Langley Research Centers, Arnold Engineering Development Center (AEDC) in Tullahoma, TN and National Full-Scale Aerodynamics Complex (NFAC) in Mountain View, CA, Air Force Research Lab (AFRL) in Dayton, OH, and Sandia National Laboratories in Albuquerque, NM.

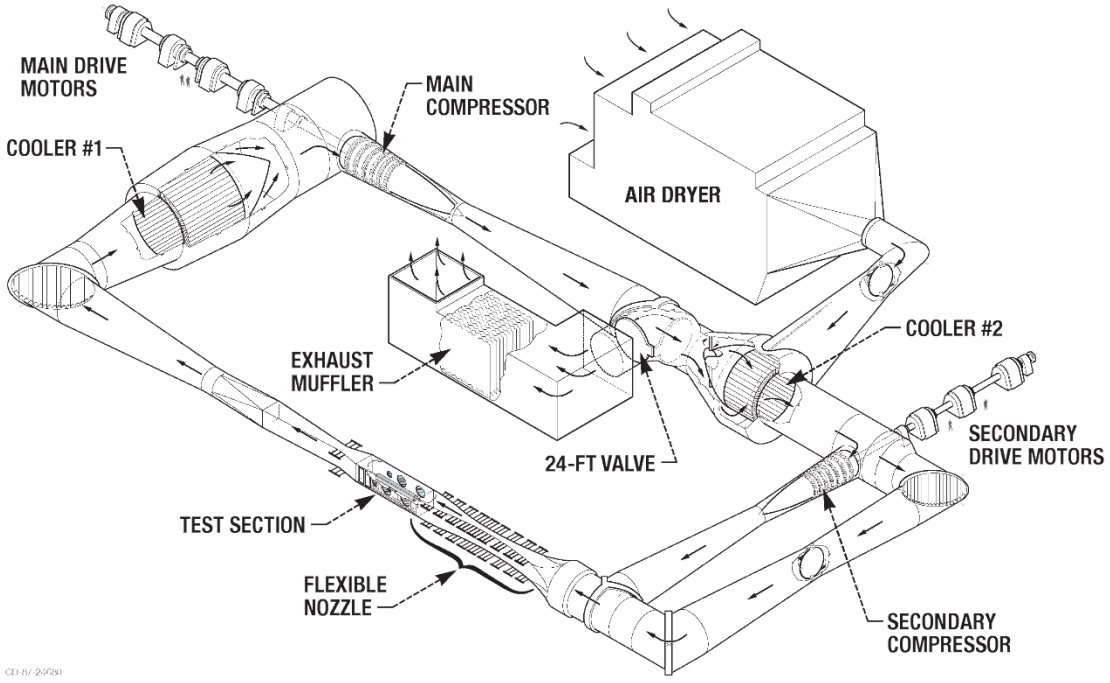

Figure 1: 10- by 10-Foot Supersonic Wind Tunnel Overview

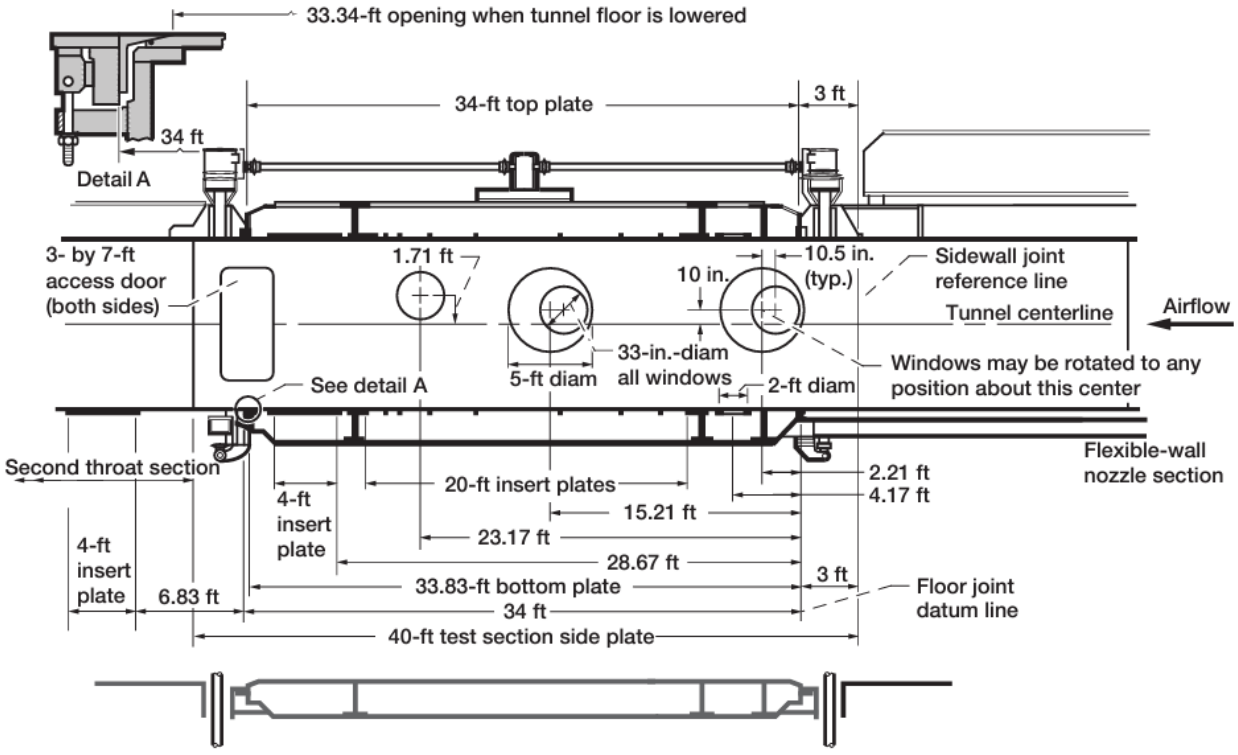

Figure 2: Elevation view of the 10- by 10-Foot Supersonic Wind Tunnel test section.

B. Previous Characterization Test Entries

The last full characterization of the 10x10 SWT occurred in 1993 and 1995 utilizing the 17-Wedge Array (Ref. [6]). Results from the full characterization were used to define operating conditions for the facility, advise customers on flow quality and uniformity in the test section, and feed into measurement uncertainty analyses of primary variables of interest, such as test section Mach and Reynolds number. The results of the bottom-up uncertainty analysis on this calibration data set allowed for the wind tunnel characterization team to determine leading contributors to the uncertainty estimates. Although not the primary purpose of this report, the use of MUA results and recommendations to direct changes for future characterization efforts is important and applicable in this case, as discussed in Ref. [7].

Between 1995 and the present, there have been periodic characterization efforts, some of which were for specific portions of the facility operating envelope with the 17-Wedge Array and some were check calibrations of the test section flow field using the smaller 5-Wedge Array. The most recent check calibration occurred in 2014 (Ref. [8]). The results of the check calibrations indicated the existing tunnel calibration continued to produce consistent test results compared to what was observed in the 1993/1995 test entries. The upcoming changes to the facility in 2024/2025, including an update to the tunnel control system, replacement/upgrade of the primary data acquisition system, and upgrade of the ESP 8400 System to Optimus, require that the facility undergo a full characterization to define updated calibration relationships, changes to the flow quality, uniformity, stability, etc., and to capitalize on opportunities to reduce uncertainty estimates for test section variables of interest, such as Mach and Reynolds number.

IV. 10x10 SWT Characterization Array Overview

The following section is intended to be a brief overview of the design of the 10x10 SWT Characterization Array (a thorough discussion of the design choices made will be included in a future NASA Contractor Report (CR)). The frame of the 10x10 SWT Characterization Array is a 5-ft by 5-ft square with support struts, each of which include probe mounting points, at every 45 degrees. There are a total of 57 probe locations on the array frame, 56 of which are identical mounting patterns to allow for probe interchangeability while the central mount is unique to the Variable-Angle-Wedge (VAW) probe. The array frame is intended to mount to either a fixed-sting in the facility lower strut or the 96-inch Translation System, an existing model translation system built in 2002. The array has been designed to survey the test section of the 10x10 SWT across the full operating envelope of the facility, including tunnel air heater conditions which reach stagnation temperature of 1140 R.

As shown in the diagram in Figure 3, there are a variety of flow sensing probes which were included in the design of the hardware. There is a single variable-angle-wedge probe at the center of the array capable of varying its half-angle from 14 to 29 degrees to measure the local Mach number through the ratio of the post-oblique, post-normal-shock total pressures ($P_{T,4}$), as measured by pitot tubes parallel to the wedge faces, and post-normal-shock total pressure ($P_{T,2}$), as measured by pitot tubes parallel to the freestream flow (see Ref. [9] for details on VAW probe operating principles). There are twelve of each of the following probe types: 1) 5-hole 20-degree-half-angle cone probes and 2) 10-degree-half-angle, conical-tip pitot-static probes. Both probe types acquire an independent measurement of Mach number (Ref. [2]) and the cone probes measure two components of flow angularity, as opposed to the one component of flow angle measured by a supersonic wedge probe. There are a total of 30 total temperature probes in the arrangement of probes. The total temperature measurements are made by a tip-sensitive Class-A RTD element which is thermally insulated by a ceramic sheath within the aspirated-tip probe housing. A more robust, high-temperature version of these probes exist for tunnel air heater testing. Two dynamic wedge probes were designed and built for the array, as well, each of which contain six Kulites: 2 installed flush in the 20-degree half-angle wedge faces, two oriented to face into the flow parallel to the wedge faces, and two measuring post-normal shock total pressure. All probe types listed above are aligned with their tips or wedge vertices at a common measurement plane except for the pitot-static probes whose static ring is aligned with the measurement plane. There are unique mounting points outside of the probe types mentioned above for up to five gas sensing probes to characterize the gas composition in the test section during tunnel air heater testing (see Ref. [10] for previous vitiated air studies in the 10x10 SWT).

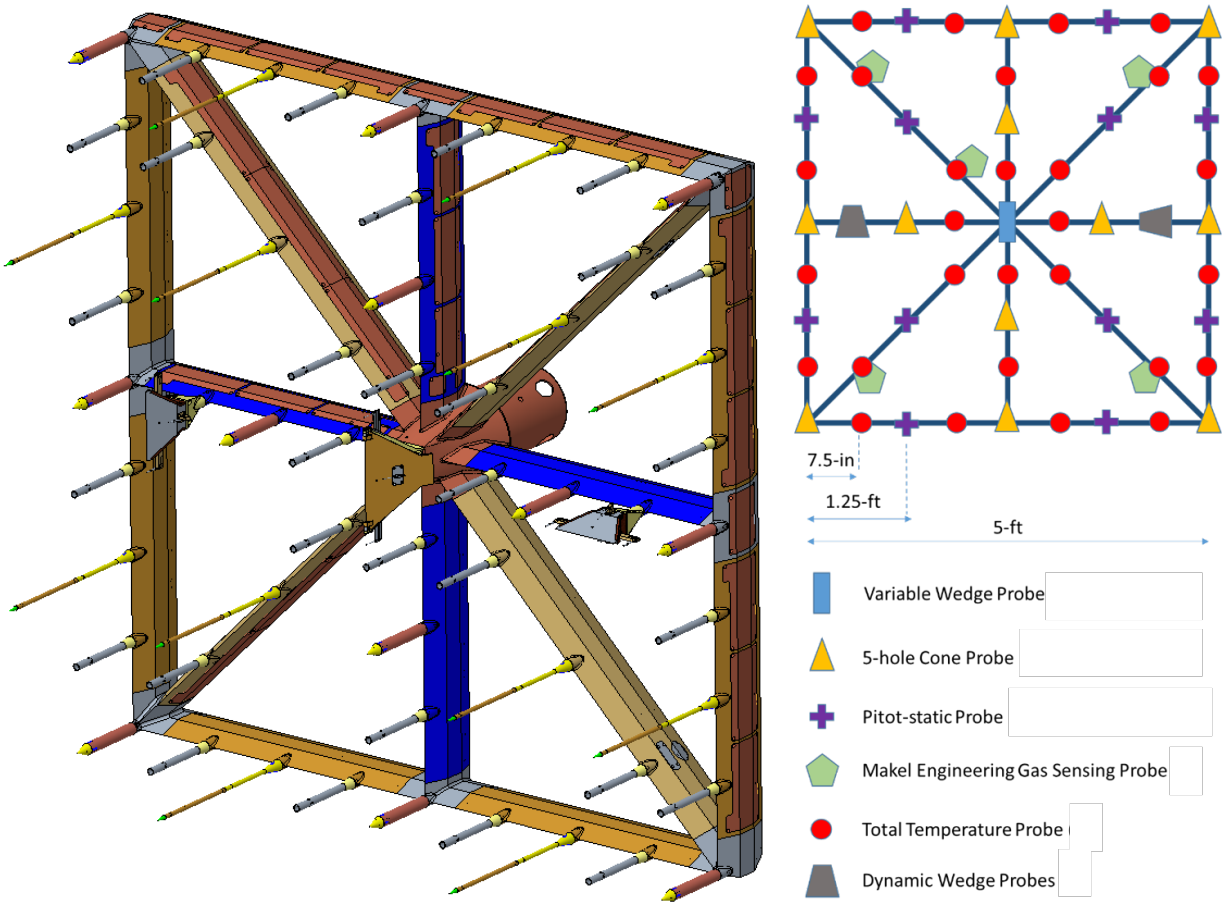

Figure 3: Overview of the 10x10 SWT Characterization Array and typical instrumentation arrangement.

V. CFD-Influenced Design Choices

The full design process for the 10x10 SWT Characterization Array involved dozens of design choices, many of which will be discussed in a future NASA CR. This section will discuss several situations in which CFD simulations were advantageous to validate design choices, promote changes to the existing design, or support future use of the array and its various probe types.

A. Pitot-Static Probe Sizing & Probe-to-Probe Spacing

Pitot-static probe sizing recommendations from Reference 1 are very common, however, due to the potential error in the measurement of freestream static pressure due to flow recovery from the tip or back-pressuring from support struts, it is advantageous to double-check these rules-of-thumb for exact flow conditions (Mach and Reynolds number) and probe and support geometry. As suggested in Reference 1, the static ports on the pitot-static probes are located 16 probe diameters downstream of the shoulder of the 10-degree half-angle conical tip, and the static ports are located 8 support strut diameters upstream of the shoulder at which the array frame's 10-degree half-angle leading edge meets the 1.5-inch constant thickness portion of the frame. To avoid probe-to-probe interference, relatively simple oblique shock relations were calculated or looked up in Ref. [11] to determine initial probe separation distances.

The CFD simulation cases performed to validate the flow recovery distances along the static probe and probe-to-probe spacing are shown in Table 1. The flow conditions were chosen to represent the current corners of the Mach and Reynolds number operating envelope. The geometry used in the simulations and examples of the simulation results, particularly the shock patterns generated, can be seen in Figure 4. The shock patterns for Mach 2.0 conditions (middle image in Figure 4) indicate that the oblique shocks generated by the pitot-static probe intersect the adjacent total temperature probes downstream of the aspiration holes. The flow through the temperature probes' aspiration holes on the side nearest the pitot-static probe does not appear to be changed due to the presence of the intersecting oblique shock, thus removing concerns that the probe performance will be altered due to probe-to-probe interference.

Table 1: Conditions performed during simulations of 3-probe configuration to assess pitot-static probe sizing and probe-to-probe spacing. Volume grid cells = 76,116,619.

CASE NUMBER	MACH NUMBER [ ]	TOTAL PRESSURE [PSFA]	STATIC PRESSURE [PSFA]	REYNOLDS NUMBER [10^6/FT]	TOTAL TEMPERATURE [R]	TOTAL ITERATIONS
1	2.0	200.1	25.578	0.34	560.0	800
2	3.5	200.2	2.625	0.11	729.6	1477
3	2.0	2066.3	264.079	3.50	560.0	2948
4	3.5	4721.4	61.901	2.50	729.6	1515

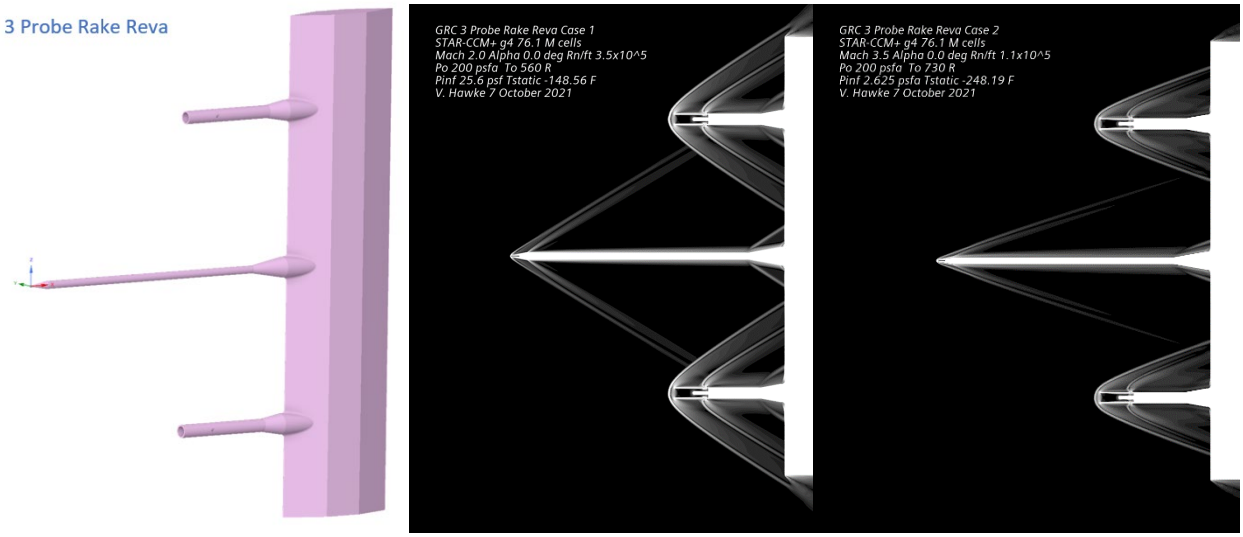

Figure 4: Geometry of 3-probe simulation, including a pitot static probe and two adjacent total temperature probes (left), and examples of flow field simulation results at low Reynolds number conditions in the 10x10 SWT at Mach 2.0 (middle) and 3.5 (right).

The static pressure profile along the surface of the pitot-static probe is shown for all four test cases from Table 1 in Figure 5 as the percent difference in surface static pressure from freestream static pressure. The profile shows the typical static pressure rise when passing through the oblique shock at the conical tip and expansion over the conical shoulder. The flow then recovers towards freestream static pressure as it moves downstream along the constant-diameter section of the probe body. The static pressure profiles show indications of back-pressuring as the flow approaches the rake body. For the Mach 2.0 conditions, the static pressures along the probe length approach values of less than 0.25% deviation from the freestream static pressure. At Mach 3.5 conditions, the pressure profile on the probe takes longer to recover to similar levels of deviation, particularly at the 2.5e6/ft Reynolds number condition. However, when this information is put into engineering units, the largest difference between the static pressure at the static port location and the freestream static pressure is on the order of 0.002 psi. Given that the pressure transducers planned for use with this hardware are 15-psid units with 0.05% of full-scale (F.S.) accuracy, the potential error/bias due to probe sizing is a fraction of the uncertainty in the instrument making the measurement.

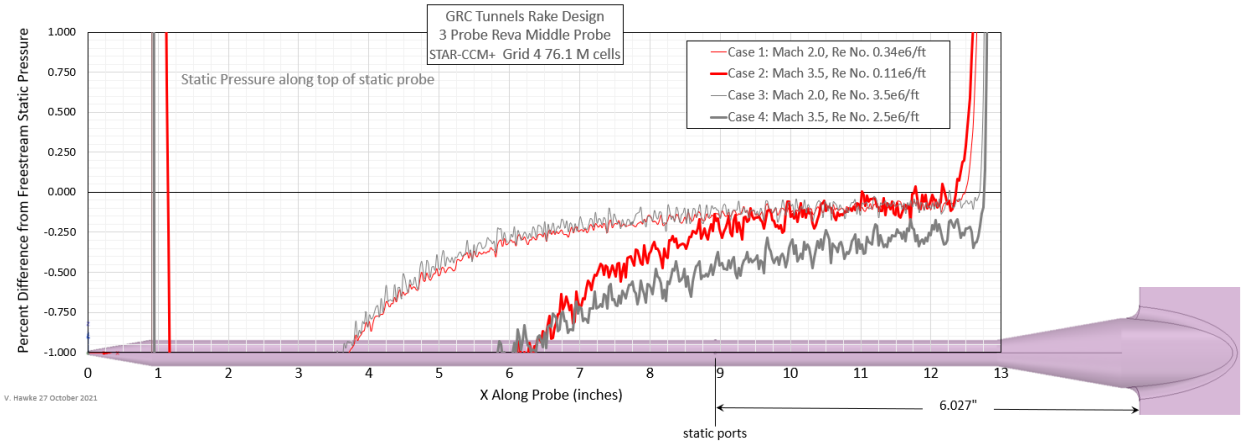

Figure 5: Static pressure profiles along surface of pitot-static probe at four flow conditions.

B. Variable-Angle-Wedge Probe Oblique Pitot Location

The location of the oblique pitot tubes, the pitot tubes oriented parallel to the wedge surfaces, on the VAW probe is critical to ensuring a proper estimation of freestream Mach number. Preliminary oblique shock relations for a wedge (Ref. [11]) and experience with the 17-Wedge Array's supersonic wedge probe design (Ref. [6]) led to an initial design for the VAW probe. To validate this design choice, the full geometry of the VAW probe, including the center-body of the characterization array, was simulated at four unique flow conditions, as shown in Table 2, to simulate the extents of the 10x10 SWT operating envelope. The VAW probe half-angle was set to 16.5 degrees for the Mach 2.0 simulations and 23.5 degrees for the Mach 3.5 simulations, both angles chosen to be near the half-angle which produces the peak in the ratio of VAW probe pitot pressures ($P_{T,4}/P_{T,2}$).

Table 2: Conditions performed during simulations of the Variable-Angle-Wedge probe for oblique pitot tube placement validation. Volume grid cells = 149,504,728 for Cases 1 & 3; 168,871,345 for Cases 2 & 4.

CASE NUMBER	MACH NUMBER [ ]	TOTAL PRESSURE [PSFA]	STATIC PRESSURE [PSFA]	REYNOLDS NUMBER [10^6/FT]	TOTAL TEMPERATURE [R]	TOTAL ITERATIONS
1	2.0	200.1	25.578	0.34	560.0	435
2	3.5	200.2	2.625	0.11	729.6	310
3	2.0	2066.3	264.079	3.50	560.0	1000
4	3.5	4721.4	61.901	2.50	729.6	1452

The placement of the oblique pitot tube had to remain above the boundary layer developing along the wedge surface, below the oblique shock generated by the wedge vertex, and free from other disturbances which would prevent the pitot tube from accurately measuring $P_{T,4}$. The initial design succeeded in avoiding placing the pitot tube in the boundary layer or outside of the oblique shock from the wedge vertex, however, it did not take into account the disturbances generated by the hinges at the ends of the wedge vertex. The left image in Figure 6 shows the original placement of the oblique pitot tubes along the wedge face being much too far aft along the wedge surface; at Mach 2.0, shocks generated by the hinges on the VAW probe cross upstream of the oblique pitot tubes and cause an unexpected loss in the expected $P_{T,4}$ value. A modification to the oblique pitot tube position and an increase in the height of the wedge allowed for the shock pattern generated by the VAW probe hinges to cross downstream of the pitot tube at Mach numbers of 2.0 and above. Figure 7 shows examples of the shock patterns on the VAW probe's vertex and oblique pitot tubes for the modified design, confirming the oblique pitot tube placement is sufficiently separated from the wedge face and the oblique shock from the wedge vertex to avoid influencing the $P_{T,4}$ measurement.

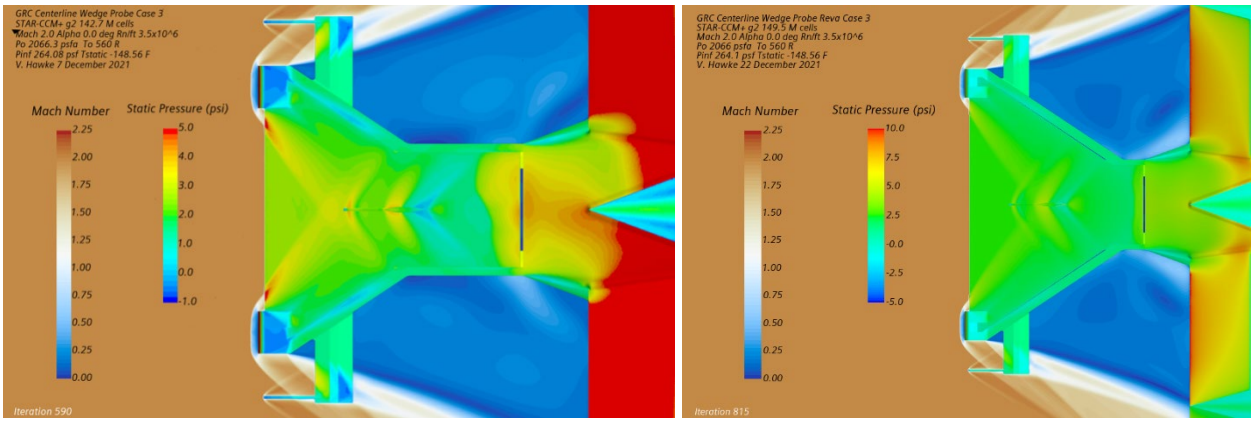

Figure 6: Disturbances generated by Variable-Angle-Wedge probe hinges before (left) and after (right) modifications to design. Mach 2.0, Reynolds number 3.5x10^6 per foot conditions shown.

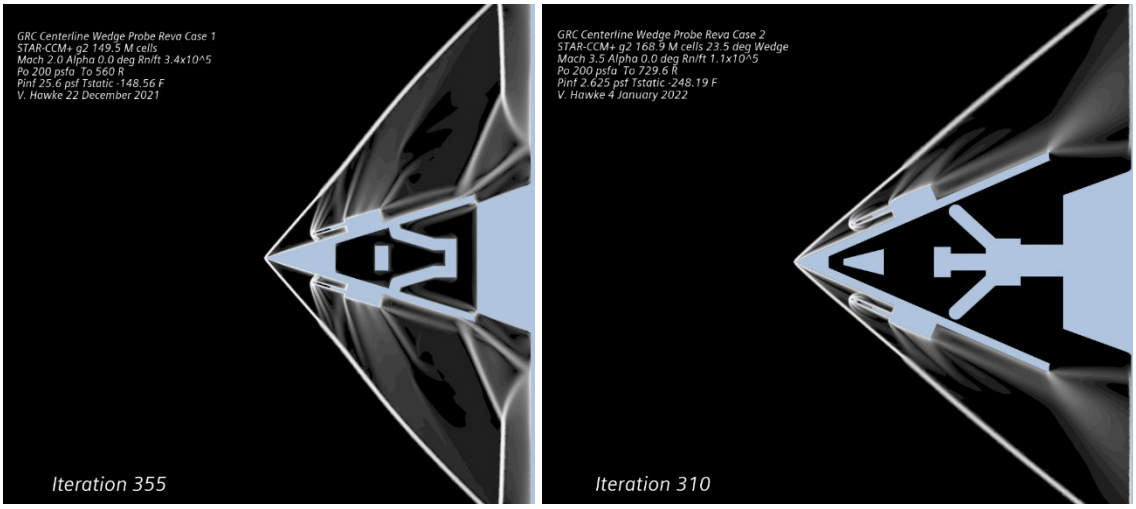

Figure 7: Shock patterns on the Variable-Angle-Wedge probe final design at Mach 2.0, wedge half-angle of 16.5 degrees, and Reynolds number 0.34x10^6 per foot (left) and Mach 3.5, wedge half-angle of 26.5 degrees, and Reynolds number of 0.11x10^6 per foot (right). Images are a planform cross-section of the probe at the centerline of the wedge.

C. Drag Estimates of the Characterization Array

During preliminary design reviews of the 10x10 SWT Characterization Array, concerns were raised over the blockage of the array within the test section. Studies have been conducted in the 10x10 SWT to identify cross-sectional blockage levels which would inhibit the tunnel's ability to start at various Mach numbers (Ref. [12]), however, there are other criteria to be considered. The drag coefficient, therefore, the profile and shape factor of the model, is considered as a predictor variable in the tunnel starting process in Figure 6 of Reference 13. To get an estimate of the drag coefficient on the model, CFD simulations were performed of the array frame and all probes installed in the positions defined in Figure 3. An example of the resulting flow field over the simulated model is shown in Figure 8. With a dynamic pressure of 71.68 psf, the simulation resulted in a drag load of 375 lbf and a model cross-sectional area of 805.13 in^2. The resulting coefficient of drag, C_d, is then 0.936 for the array. Based on previously documented boundary layer characteristics of the facility (Ref. [14]), the boundary layer height will be assumedly 8 inches on each surface of the facility for purposes of this correlation. Using Figure 6 from Reference 13, the ratio of model blockage area to core test section area (7.44%) and a C_d of 0.936 lead to the conclusion that starting the facility at Mach 2.0 may be challenging as this data point falls very close to the permissible frontal area curve for this drag coefficient. As

is common in the 10x10 SWT, the starting Mach number can be increased to start the tunnel with larger blockage models, which, based on this analysis, should be plausible, as well.

Figure 8: CFD simulation of 10x10 SWT Characterization Array for drag estimation at Mach 2.0, Reynolds number 0.34 x 10^6 per foot.

D. CFD-Characterization of 5-hole Cone Probes

The 10x10 SWT Characterization Array, as mentioned previously, will use twelve 5-hole cone probes to measure local Mach number and two components of flow angularity. Taylor-Maccoll solutions could be used to predict the average cone surface pressure (P_c) for a given cone half-angle cone and freestream Mach number, thus allowing a relationship between the ratio of $P_c/P_{T,2}$ and the freestream Mach number to be used. To improve the fidelity of the Mach number estimations, as-built geometry of the cone half-angle, freestream Reynolds number, and incident flow angle on the cone probe were investigated as predictor variables. Similarly, the estimation of flow angle components measured by the cone probes is expected to require a similar amount of predictor variables to measure the flow angularity in the wind tunnel to an acceptable level of accuracy.

There are multiple methods available for characterization of these types of probes: 1) in-situ calibration in the 10x10 SWT, 2) calibration in a small-scale supersonic wind tunnel or free jet facility, and 3) CFD simulation. The first method, in-situ calibration in the 10x10 SWT, is by far the most expensive method given the cost to operate a large wind tunnel facility and the additional hardware required to properly orient and roll the probes within the test section. The use of small-scale facilities to characterize flow sensing probes for larger tunnels is common practice, however, the cost required to sufficiently characterize twelve probes individually at various combinations of Mach number, Reynolds numbers, and probe orientations becomes appreciable[6]. As a compromise, the following method has been proposed to characterize the 5-hole cone probes for the 10x10 SWT Characterization Array: perform CFD simulations across a range of Mach & Reynolds number combination, cone half-angle geometry, and incident flow angles to develop regression models from pressures sampled at as-designed port locations. CFD simulations do come at a cost, however, funding for the simulations were provided by the AETC CFD Wind Tunnel Integration Project, therefore the NASA Glenn Wind Tunnel characterization team did not incur any additional cost. Additionally, such simulations could be performed in tandem with the final phases of the design effort and hardware fabrication, shortening the time until the cone probe regression models would be available for use in the 10x10 SWT. To validate the regression models formed via CFD results, a short set of tests with a small sample size of the 5-hole cone probes is suggested, as well.

[6] The small-scale facilities considered for characterization of the cone probes were non-AETC facilities within NASA Glenn Research Center, therefore the cost of facility occupancy and power would fall upon the customer to pay.

A design of experiments (DOE) methodology was used to select the 70 combinations of conditions to simulate; 21 condition combinations were chosen using a central-composite-design (CCD), 40 with a space-filling design, and 9 condition combinations were randomly chosen as validation simulations. Figure 9 shows the 61 conditions within the design space selected for developing the regression models to estimate Mach number and two components of flow angularity from the 5-hole cone probes. Conditions are based upon the full operating envelope of the 10x10 SWT, including conditions that could be pursued in future characterization efforts. The CFD simulations, at the time of writing this report, have converged upon solutions that appear representative of the physics present in the flow over the cone probe. Regression models for Mach number and flow angle prediction are being generated, lessons learned on the CFD process are being documented, and follow-on validation tests of the regression models are being planned in NASA Glenn test cells. A follow-up report is anticipated to provide more detail of the simulations and planned validation efforts.

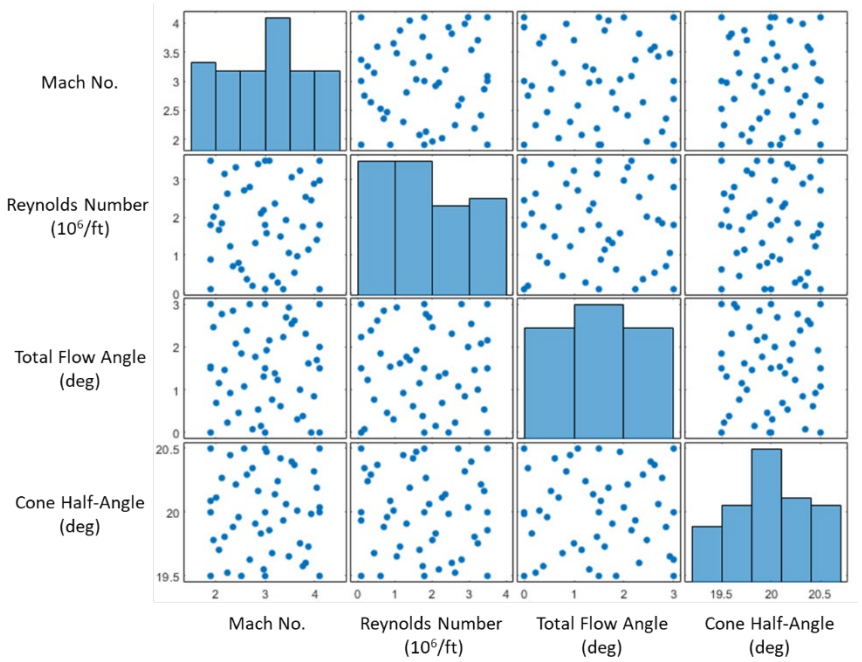

Figure 9: Design space and condition combinations selected for the CFD-characterization of the 10x10 SWT Characterization Array's 5-hole cone probes. Validation points not shown.

Future work could include investigations of the uncertainty involved in performing probe calibrations in the method described in this section. Factors such as grid density and turbulence model choice could be incorporated into the DOE approach to assess variation in results caused by the simulation parameters. If the wind tunnel characterization team decides to use the cone probe CFD-calibration results in the process of developing wind tunnel calibration relationships, the estimation of CFD-related uncertainty will become mandatory to properly estimate uncertainties in primary variables of interest for the 10x10 SWT.

VI.Conclusion

The development of the 10x10 SWT Characterization Array and its suite of probe types would have been possible with typical design methods and rules-of-thumb, however, the use of CFD simulations to validate design choices has proven to be useful to improve the understanding of the data quality expected from the various probe types during future wind tunnel characterization efforts. Potential unanticipated sources of biases in future measured data can be avoided through CFD validation of seemingly simple design choices for typical probe types. Integration of CFD in wind tunnel hardware development, particularly hardware intended for wind tunnel characterization, is expected to be an activity that continues and becomes increasingly more common place.

VII.Acknowledgments

The authors would like to thank the NASA Aerosciences Evaluation and Test Capabilities (AETC) Portfolio Office for support of wind tunnel characterization practices across the agency and the CFD and Wind Tunnel Test Integration project. We would also like to thank the designer on the 10x10 SWT Characterization Array, Don Morr, for his efforts to incorporate input from the CFD analyses into this hardware design and produce a robust piece of characterization hardware. We would also like to acknowledge Jim Ross (NASA Ames Research Center) for his willingness to support these types of efforts in the 10x10 SWT and across the NASA wind tunnel community through the AETC-funded CFD and Wind Tunnel Test Integration project. Finally, we would like to thank the NASA Glenn Research Center testing division and TFOME II engineering management for their continuous support in furthering the understanding and characterization efforts within our ground-test facilities and mentoring the next generation of engineers at the center.

References

[1] Reed, T.D.; Pope, T.C.; and Cooksey, J. M.: Calibration of Transonic and Supersonic Wind Tunnels. NASA CR-2920, 1997.

[2] Hill, J.A.F.; Baron, J.R.; Schindel, L.H.; and Markham, J.R.: Mach Number Measurements in High-Speed Wind Tunnel. AGARDograph 22, 1956.

[3] Pope, A.: Wind Tunnel Calibration Techniques. AGARDograph 54, 1961.

[4] Varner, M. O.: Corrections to Single-Shielded Total Temperature Probes in Subsonic, Supersonic, and Hypersonic Flow. AEDC-TR-76-140, 1976.

[5] Soeder, Ronald H.; Roeder, James W.; Linne, Alan A.; and Panek, Joseph, W.: User Manual for NASA Glenn 10- by 10-Foot Supersonic Wind Tunnel. NASA/TM-2004-212697, 2004.

[6] Arrington, E. A.; Spera, D.A.; and Blumenthal, P.: Calibration of the NASA Glenn Research Center 10- by 10-ft Supersonic Wind Tunnel (1993 and 1995 Tests). NASA/TM-2000-209799, 2000. http://ntrs.nasa.gov

[7] Johnson, Aaron M.; Kelsey, Nathan D.; Poljak, Pamela L.; and Rinehart, David A.: Uncertainty Improvements in the NASA Glenn Research Center 8- by 6-Foot Supersonic Wind Tunnel. AIAA AVIATION 2023 Forum. http://arc.aiaa.org | DOI: 10.2514/6.2023-4367.

[8] Johnson, A.; Pastor-Barsi, C.; and Arrington, E.A.: Check Calibration of the NASA Glenn 10- by 10-Foot Supersonic Wind Tunnel (2014 Test Entry). NASA/CR-2016-218894, 2016. http://ntrs.nasa.gov

[9] Maxwell, H.; and Hartley, M.S.: Aerodynamic Calibration Results for the AEDC-PWT 16-ft Supersonic Tunnel at Mach Numbers from 1.50 to 4.75. AEDC-TR-69-102, 1969.

[10] Cubbison, Robert. W.; Meleason, Edward T.: Water Condensation Effects of Heated Vitiated Air on Flow in a Large Supersonic Wind Tunnel. NASA TM X-1636, 1968. http://ntrs.nasa.gov

[11] Ames Research Staff: Equations, Tables, and Charts for Compressible Flow. Report 1135, 1953. http://ntrs.nasa.gov

[12] Pastor-Barsi, Christine; Peters, Christopher; and Vyas, Manan: Summary of the 2017 Blockage Test in the 10- by 10-Foot Supersonic Wind Tunnel. NASA/TM-2018-220016, 2018. http://ntrs.nasa.gov

[13] Czysz, Paul A.: Correlation of Wind Tunnel Blockage Data. ASD-TDR-63-230, 1963.

[14] Smith, Larry E.; Blumenthal, Phillip Z.; Cubbison, Robert; and Baskin, Kenneth: Data and Supporting Documentation from the 10x10 SWT Test Section Calibration Test – August 28-October 31, 1991. Preliminary Information Report #29, 1992.